Investigation of UPQC for Sag Compensation in Wind Farms to Weak Grid Connections ⋆

M.F. Farias *, **P.E. Battaiotto** *, **M.G. Cendoya** *,

* *Facultad de Ingeniería, Universidad Nacional de La Plata, CC91, La Plata, Argentina*
tel/fax: +54 221 425 9306
e-mail: marcelo.farias@ing.unlp.edu.ar, pedro@ing.unlp.edu.ar, cendoya@ing.unlp.edu.ar

Submitted: 30/04/2010
Accepted: 12/06/2010
Appeared: 30/06/2010

Abstract:
In the last years, the wind power generation incorporated into standard grids has been increased significantly. This situation forced the revision of grid connection code requirements, to guarantee the reliability in systems with high wind power penetration.
In case of events like voltage sags, wind farms must keep connected to power system avoiding power imbalance and even system collapse. For induction generator based wind farms connected to weak grids, such sag may lead to wind farm outage.
Several strategies have been proposed in the literature, but often for full or partial amplitude voltage restoration, without caring phase jump associated to voltage sags.
In this work a voltage sag compensation strategy is proposed for voltage magnitude restoration with phase jump compensation, and compared with a magnitude–only restoration strategy. These strategies were implemented using a Unified Power Quality Compensator UPQC. A model of wind farm with induction generators connected to a weak grid system, including a detailed UPQC compensator was developed on simulation software. Then simulations were conducted in order to compare the proposed compensation strategy with previous methods.
Results show a better wind farm performance in proposed strategy than that found in magnitude only compensation schemes. Also, the power rating of the compensators used in the proposed strategy is similar than the one that would be required in classical strategies.
Thus, considering the improvement in performance, the proposed strategy is recommended in retrofitting the existing installed fixed speed induction generators based wind farms.

Keywords: Voltage sag, Power quality, Low voltage ride through, Wind farm, UPQC, Phase jump

1. INTRODUCTION

In the past, the penetration of wind energy into the electric power system was low. Then, in case of grid faults, the wind farms were simply disconnected without consequences on system stability, Palsson (2002).

In the last decades, the wind energy penetration has been increased significantly, and stills increasing. This situation forced the revision of electric utilities grid codes requirements, to guarantee the reliability in systems with high penetration levels POE 12.3 (2004), E.ON Netz (2003).

In steady–state condition, wind farms must provide ancillary services, like the conventional power plants, e. g. reactive compensation, voltage and frequency regulation, etc; in transient conditions, wind farm must withstand several types of disturbances coming from the grid, such as voltage sags, swells, unbalances, etc., keeping the connection to the power system to avoid power unbalance and even system collapse.

In case of balanced three–phase short–circuit occurrence, voltage sags may be observed near the point of failure, and characterized by a sudden voltage reduction and lagging phase jump. For induction generator based wind farms such sag may lead to wind farm outage, due to reactive power needed to restore the internal magnetic flux once the fault is cleared. So, its behavior limits the **low voltage ride through** capability in this type of generators.

⋆ The authors would like to thank to *Fundación YPF*, to La Plata National University – UNLP, to National Agency of Science and Technology Promotion ANPCyT (PICT08/11-0535), and to *Comision Nacional de Investigaciones Científicas – CONICET*, by their financial support.

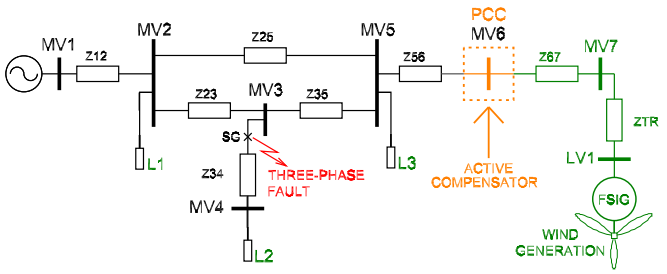

Fig. 1. Power system study case. Single line electrical diagram

In previous works, strategies have been proposed to improve such capability, but mainly concentrated on magnitude restoration of the voltage sag, whereas little attention has been paid to the phase jump.

In this work, the behavior of a wind farm with squirrel cage induction generators, connected to a weak grid and facing balanced three-phase voltage sag, is analyzed. To improve the wind farm low voltage ride through (LVRT) capability, is proposed a strategy tending to restore the voltage level and compensate the phase jump, and it is also compared with "magnitude restoration only" strategies.

The paper is organized as follows. System description and modelling is developed in Section 2. The modeling includes wind farm (turbine and generator's model) and compensator's model. Voltage sag generation at wind farm terminal is also discussed in this Section. In Section 3, the magnitude only restoration strategy is described, the proposed strategy is presented, and a series converter's rating comparison is performed. The Section 4 presents some considerations about DC bus voltage regulation. In Section 5 simulations results are presented, in order to show the wind farm behavior without compensation, and the performance of both strategies. Also is showed in this Section, series generated voltage and shunt current for comparison purposes, and DC-link voltage regulation.

2. SYSTEM DESCRIPTION AND MODELLING

2.1 Power system description

The electrical power system under study is composed by a wind farm connected to a weak distribution network. This system is taken from a real case, Saad-Saoud (1998). Fig.1 shows a single line electrical diagram of power system.

The wind farm generation facility is composed by a total of 36 fixed-speed induction-generator based wind turbines, adding up to 21.6MW. Each turbine has attached a 175kVAr compensation capacitor bank, and it is connected to the distribution grid by means of a 0.69/33kV, 630kVA transformer.

As seen in Fig.1, MV1 represents the infinite bus, and there are three loads in MV2, MV4 and MV5 buses. Distribution grid nominal voltage is 33kV.

The ratio between short circuit power at the point of common coupling (PCC) bus (MV6) and wind farm rated power, give us an idea of the "connection weakness". Thus considering that the value of short circuit power at MV6 bus is $S_{SC} \simeq 120MVA$, this ratio can be calculated:

$$r = \frac{S_{SC}}{P_{WF}} \simeq 5.5$$

Values of $r < 20$ are considered as a "weak grid" connection, see Ledesma (2003).

2.2 Model of wind farm

A complete model of the wind farm is obtained by **turbine aggregation**; this implies that the whole wind farm can be modeled by only one equivalent wind turbine, whose power is the arithmetic sum of the power generated by each turbine P_i.

$$P_i = \frac{1}{2} \cdot \rho \cdot \pi \cdot R^2 \cdot v^3 \cdot C_P \qquad (1)$$

$$P_T = \sum_{i=1\cdots36} P_i$$

Where ρ is air density, R the radius of the swept area, v the wind speed, and C_P the power coefficient. In the study case this values are $R = 31.2\,m$, $\rho = 1.225\,kg/m^3$, and C_P values are taken from a widely used classical model, Tai-Her (2008). The boundary layer effect and turbulence effect on wind speed are neglected, as usual in models employed in many publications, Rosas (2003).

For the squirrel cage induction generator, the model available in Matlab/Simulink SimPowerSystems© libraries is used, The MathWorks (2007). It consists of a fourth–order state–space electrical model and a second–order mechanical model, Kundur (1994). Wind turbine inertia is represented as concentrated in the rotor of electrical generator.

2.3 Voltage sags

Voltage sag is a decrease in voltage level (0.1p.u. – 0.9p.u.), lasting from 0.5 cycle to 1 min. In the occurrence of three phase faults (short circuit), voltage sags are observed near the point of failure, and characterized by a sudden voltage reduction and lagging phase jump, Dugan (2002). Lagging phase–jump is due to circulating short circuit currents and inductive nature of electrical grid.

In the study case, a three phase fault is produced in MV3 bus (see Fig.1), lasting for 500ms. Voltage sag appears at the point of common coupling PCC (MV6), and it can be estimated in simplified form using phasor algebra and disregarding the wind farm generated power.

$$\begin{aligned} \textit{Voltage sag at PCC} &: 0.4pu \\ \textit{phase jump } \Delta\varphi &: -30° \\ \textit{fault duration } \Delta t &: 500ms \end{aligned}$$

This voltage sag with phase jump occurs almost instantaneously, as will be seen in Section 5.1 (Fig.11).

2.4 Active compensator model

Custom Power System devices (CUPS), like D-Statcom, Dynamic Voltage Restorer (DVR), Unified Power Quality Conditioner (UPQC), fast transfer switches, among others,

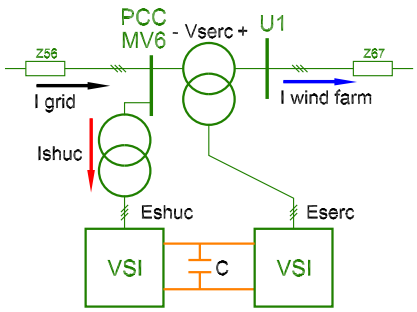

Fig. 2. Single line electrical diagram of UPQC

are devices used at distribution level to compensate flicker, improve power quality, active and reactive power control, etc. Hingorani (1995); Ghosh (2002).

The compensation action of such devices is based on three phase voltage generation, by using electronic converters of either voltage source type (Voltage Source Inverter–VSI) or current source type (Current Source Inverter–CSI). VSI converter are preferred because of its lower DC link losses and faster response than CSI converter, Ghosh (2002).

In our case, compensation strategy of voltage sag will be accomplished by using a unified type compensator UPQC. Fig.2 shows a diagram of this compensator (bus bars and impedances numbering is referred to Fig.1). The actions performed by both converters are also shown in that figure: the shunt converter (ShuC) of UPQC is responsible for injecting current I_{ShuC} at PCC, while the series converter (SerC) generates voltages V_{SerC} between PCC and U1.

An important feature of this compensator is the operation of both VSI converters (series and shunt) sharing the same DC bus, enabling active power exchange between them; this feature is exploited in the proposed strategy (see Section 3).

For the AC–side simulation model of the UPQC, both converters have been replaced by controlled voltage sources, neglecting harmonic content due to switching operation.

Based on ideas taken from Schauder (1993), the control of the UPQC is implemented in a rotating frame using Park's transformation, also called *synchronous reference frame control*. The use of Park's transformation allows the alignment of the rotating reference frame with the space vector corresponding to fundamental positive sequence PCC voltages. To accomplish this, a reference angle θ synchronized with this vector is needed. This reference angle is obtained using a Phase Locked Loop (PLL) system. In this work, a PLL based on the "instantaneous power theory *pq*", has been implemented , Akagi (2007); Sasso (2002). Such PLL–pq system features a fast tracking of space vector voltage phase angle, even under voltage variation like unbalance, swells, sags, waveform distortion, etc. .

Thus, measured phase voltages and line currents $[a, b, c]$ are transformed to the rotating synchronous reference frame $[d, q, 0]$. Positive sequence magnitudes becomes "*DC values*" in this frame, simplifing the controller design. Then, the calculated controller action in rotating frame is transformed to $[a, b, c]$ frame, using Park's inverse transformation.

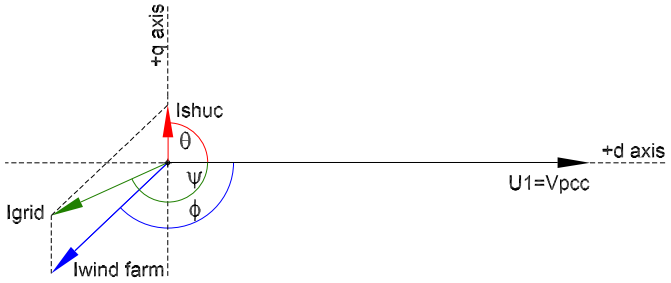

Fig. 3. Space vector diagram. Pre-sag condition

The DC–side model of the UPQC is based is the followings equations:

$$\dot{v}_{DC} = \frac{1}{C} \cdot i_{cap} \tag{2}$$

$$v_{DC} \cdot i_{cap} = p_{SerC} - p_{ShuC} \tag{3}$$

where p_{SerC} and p_{ShuC} represent the instantaneous electrical power of series converter and shunt converter, respectively.

3. VOLTAGE SAG COMPENSATION STRATEGIES

In previous works, strategies using UPQC had been proposed to improve LVRT capability of wind farms Jayanti (2006), but mainly concentrated on magnitude restoration of voltage sags, whereas no attention has been paid to phase jump.

This phase jump usually do not affect induction generator operation, but may cause tripping of equipment and auxiliary devices, like contactors, battery chargers, etc., leading to wind farm power outage.

In the following subsections, a classical full voltage restoration strategy is described, the proposed full voltage restoration with phase compensation strategy is presented, and series converter generated voltage comparison is conducted.

3.1 Full voltage restoration

In the Fig.3 is shown a steady state space vector diagram of PCC voltages, representing the nominal operating condition of the power system prior to the occurrence of the fault (pre–sag condition).

The PCC voltage level is normal, so series converter injected voltage is zero. In that diagram, the shunt converter is generating reactive power (I_{ShuC} leading V_{pcc}).

During voltage sag, the fast tracking action of PLL–pq system aligns almost instantaneously the reference frame with the reduced vector voltage at PCC. The series compensator restores the amplitude of wind farm terminal voltage, generating in–phase voltage, but phase jump is not compensated at U1 bus bar. The Fig.4 shows this action using a space vector diagram.

In the figure is clearly observed that the phase angle of electrical current is suddenly reduced due to phase jump.

$$\phi' = \phi - \Delta\varphi$$

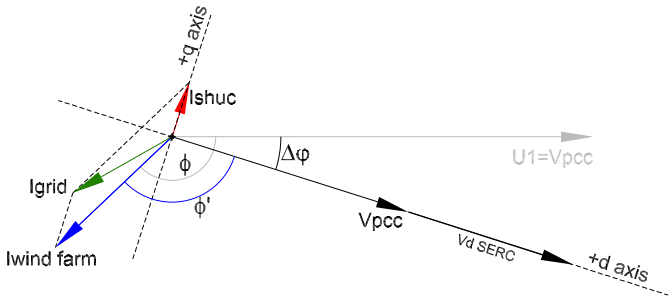

Fig. 4. Space vector diagram: Full voltage restoration

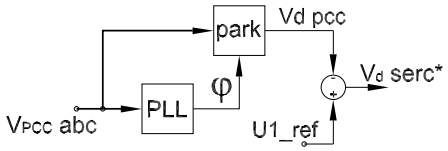

Fig. 5. Voltage restoration. Block diagram

Therefore, a transient phenomenon in electrical currents I_{abc} will occur, until pre–sag angle phase value ϕ is reached.

The reference voltage calculation for injected V_{SerC} voltages, is showed in the block diagram of Fig.5.

3.2 Full voltage restoration with phase compensation

If, in addition to voltage restoration phase jump compensation is included, transients in electrical currents, and tripping of auxiliary devices of wind farm facilities will be avoided.

To implement this strategy, it is necessary to quantify the value of the phase jump; this is achieved by the use of two PLL-pq systems. One of them, with a fast time response, is responsible of instantaneous synchronization with PCC voltage vector (this PLL is also used in the current control loop of the shunt converter in Section 4). The other one, with slower response, transiently "holds" the initial phase jump angle.

The phase jump $\Delta\varphi$ at wind farm terminals, is calculated using the following equation:

$$\Delta\varphi = \varphi_{fast}^{PLL} - \varphi_{slow}^{PLL} \tag{4}$$

Then, series converter reference voltages are calculated using Eqn.4 and Eqn.5.

$$\begin{aligned} {V_{SerC}^{d}}^{*} &= U1_{ref} \cdot \cos\Delta\varphi - V_{PCC} \\ {V_{SerC}^{q}}^{*} &= U1_{ref} \cdot \sin\Delta\varphi \end{aligned} \tag{5}$$

The control block diagram for ${V_{SerC}^{d,q}}^{*}$ reference calculation, and the vector at initial compensation action, are shown in Fig.6 and Fig.7 respectively.

In the proposed strategy, the phase compensation $\Delta\varphi$ is not maintained during voltage sag. It decreases with time towards zero, as slower PLL reaches steady–state phase angle (the same phase angle as fast PLL). Fig.8 shows this situation.

Hence, the phase angle of wind farm terminal voltage evolves in a controlled manner from pre–sag value, towards

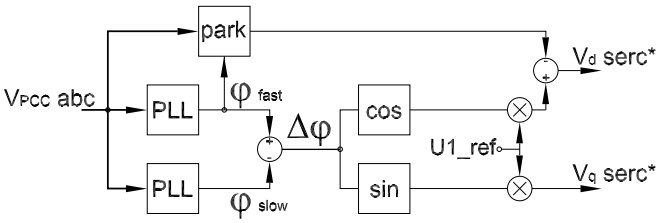

Fig. 6. Voltage restoration with phase angle compensation. Block diagram

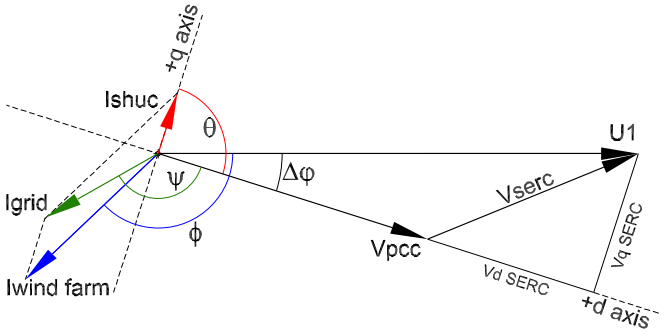

Fig. 7. Space vector diagram. Full voltage restoration with phase compensation

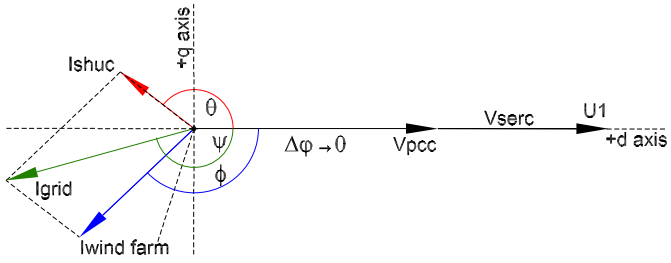

Fig. 8. Space vector diagram. Final compensation action

zero (this is, phase aligned with PCC voltage vector during voltage sag). It is also expected that electrical currents $I_{windfarm}$ remain almost unchanged.

It is necessary to note that the final condition is the same in both compensation schemes.

Additionally, the variation of the source electrical currents I_{grid} must be smoothly controlled, since rapid changes of active power injected into the grid also generate phase angle variations of voltage at PCC. A proper tuning of DC voltage controller, will allow a suitable active current injection through the shunt converter I_{ShuC}, avoiding such disturbances.

3.3 Series converter comparison

A generated voltage comparison for both strategies can be performed, using the values of voltage sag magnitude calculated in Section 2.3.

The vectors of generated voltage V_{SerC} using both strategies (Vserc I for the proposed strategy and Vserc II using full voltage restoration) are drawn in Fig.9.

The amplitude of the series converter generated voltage by both strategies can be estimated using this figure. It is

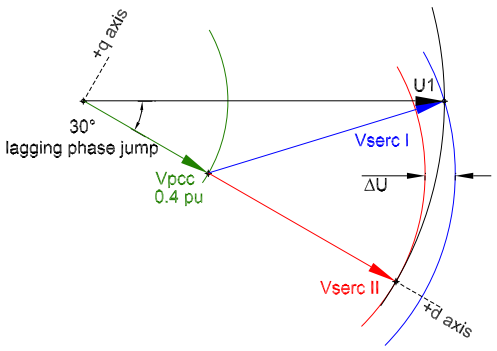

Fig. 9. Voltages generated at initial compensation action

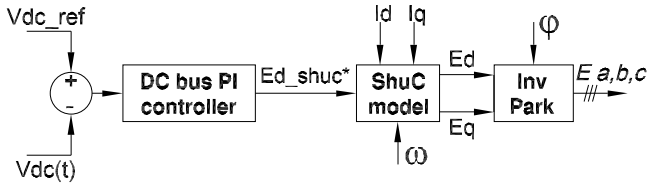

Fig. 10. DC bus voltage control. Block diagram

necessary to note that this estimation is performed at the initial instant of voltage sag.

The difference in generated voltage by the proposed strategy Vserc II seems to be $\Delta U \simeq 14\%$ larger than Vserc II.

This first approach in comparing V_{SerC} in both cases shows a small difference in generated voltages.

4. CONTROL OF UPQC DC–BUS VOLTAGE

The regulation of the DC bus voltage has been assigned to the shunt converter, injecting proper "active" currents i_{ShuC} at PCC.

In the Fig.7 can be seen that $I_{windfarm}$ and V_{SerC} vectors are not in quadrature, thus the series converter should be able to handle active power. As a result, the action of the series compensator will generate changes in the DC bus voltage.

Using the DC bus model of Eqn.2 and Eqn.3, a PI controller is implemented for the shunt converter reference voltage generation ${E^d_{ShuC}}^*$. This voltage controls directly the current I^d_{ShuC}, and therefore the active power of shunt converter p_{ShuC}. This reference voltage ${E_{d\_ShuC}}^*$ is transformed in the voltage components E_d and E_q (rotating reference frame components) using a decoupled model, Schauder (1993), and then they are transformed to phase voltages $[a, b, c]$ using inverse Park's transformation.

The Fig.10 depicts in a block diagram the DC bus voltage controller. In that figure, Id and Iq represent measured shunt converter electrical currents.

The PI controller is tuned to obtain a slow response compared with phase jump compensation dynamics, avoiding PCC voltage phase variation due to active power injection.

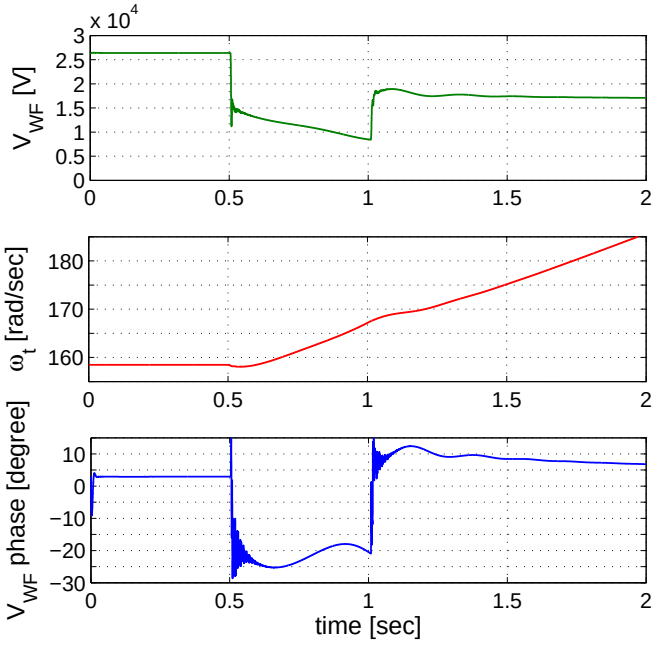

Fig. 11. WF terminal voltage, rotor speed and phase jump

It is worth noting that in the presented work, the ability of reactive power generation by the shunt converter is not used; voltage reference ${E^q_{ShuC}}^*$ is set to zero.

5. SIMULATION RESULTS AND DISCUSSION

The behavior of wind farm facing voltage sag is analyzed first; as mentioned in Section 2.3 such voltage sag is produced by a short circuit at MV3 bus bar (see fig.1). Then, both compensation strategies for the voltage sag are simulated, and performance comparison of both strategies is also conducted.

5.1 Wind Farm low voltage ride through capability

The voltage sag, with 500ms of duration time, appears at wind farm terminal reducing significantly the induction generator magnetic flux, and therefore the electromagnetic torque; the rotor speed increases almost linearly due to the action of the wind turbine torque. The wind farm terminal voltage magnitude and phase angle, and rotor speed behavior can be seen in Fig.11.

Voltage sag and phase jump values observed in simulation, are consistent with the calculated ones in Section 2.3.

$$\Delta\varphi \simeq 25°$$

The observed difference between $\Delta\varphi$ estimated in 2.3 and the simulated one, is mainly due to wind farm active power generation.

Then, once the fault is cleared, the speed of the machines is higher than before voltage sag occurrence. At this point, the reactive power required by the wind farm generators has risen due to a higher rotor slip. In case of weak grids like the one discussed here, this situation limits the voltage recovery and extends the voltage sag duration time.

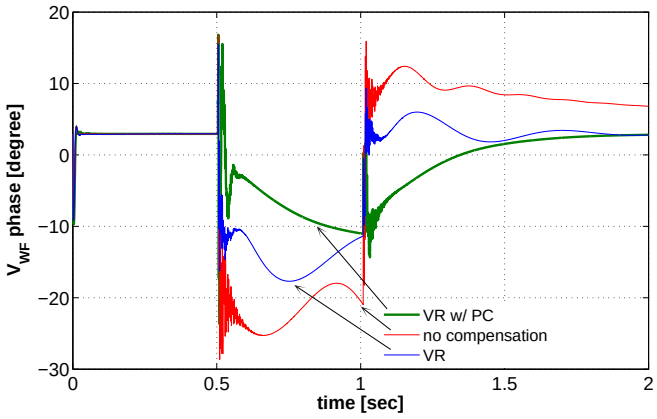

Fig. 12. Phase angle behavior at U1 bus bar.

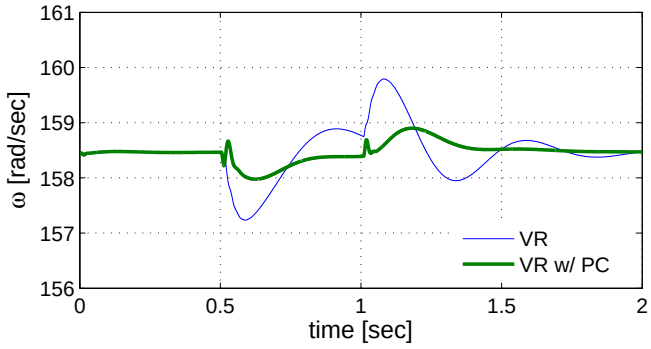

Fig. 13. WF rotor speed behavior.

It is clearly seen in the figure that wind farm speed cannot remain stable. In other words, the wind farm lacks enough LVRT capability.

5.2 Compensation of voltage sag

The strategies for voltage sag compensation presented in Section 3, were implemented and simulated using Matlab/Simulink SimPowerSystems©.

In the Fig.12, the phase angle of voltage at U1 is shown for the three simulation cases: no compensation case, voltage restoration case (VR), and full voltage restoration with phase compensation case (VR w/ PC). The high–frequency transient observed at $t = 0.5\,s$ is due to perturbed current injected at PCC. In this figure the benefits associated with the proposed strategy are seen, preventing a sudden phase jump at WF terminals, and resulting in a controlled evolution of phase angle. This behavior is also observed when the fault is cleared, and voltage tends to be restored.

The wind farm rotor speed is also benefiting from the compensation strategy. In Fig.13 the evolution of rotor speed in both cases is shown, for the purpose of comparing their behavior.

The electrical current of the wind farm also performs better in the proposed strategy, than that found in case of full voltage restoration, as is clearly seen in the lower waveform of Fig.14 showing phase current $i_a(t)$.

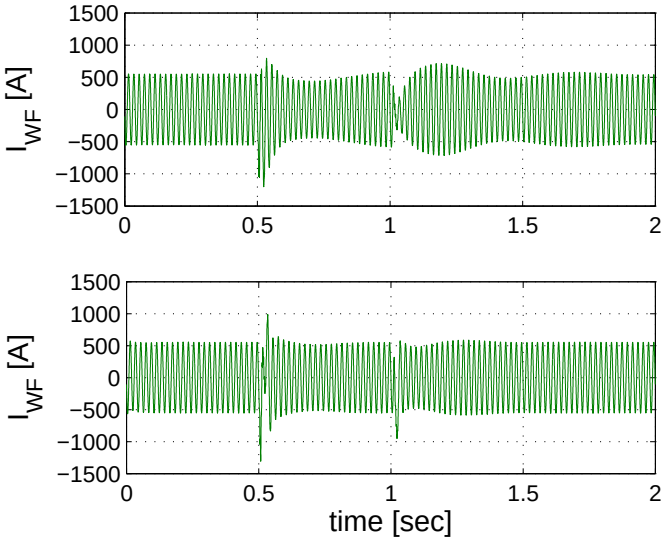

Fig. 14. Electrical current i_a behavior in classical strategy case (upper waveform) , and proposed strategy case (lower waveform)

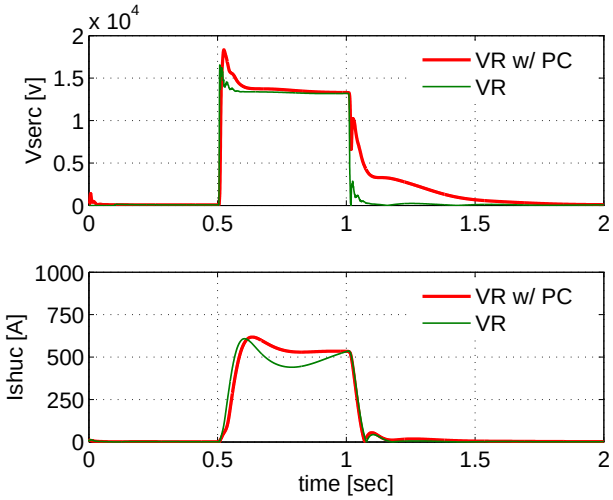

Fig. 15. Amplitude of SerC generated voltage (upper figure), and ShuC current (lower figure)

5.3 Series converter voltage and Shunt converter current

A comparison of generated voltage at the initial instant of sag occurrence is realized in the Section3.3. The upper waveform of Fig.15 shows series converter generated voltage. As expected, the generated voltages have similar amplitude in both strategies.

For the current injection I_{ShuC}, both cases have similar performance, because DC bus control tuning is the same.

5.4 DC bus controller action

As aforementioned, the DC bus voltage regulation has been assigned to the shunt converter, and the same controller has been used in both compensation schemes.

During voltage sag, the series converter injects power into the DC bus, and the shunt converter draws power from it to maintain the voltage level, as can be seen in Fig.16.

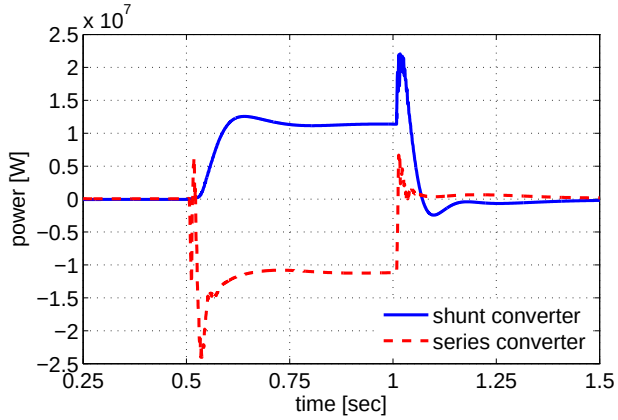

Fig. 16. Active power of series and shunt converters

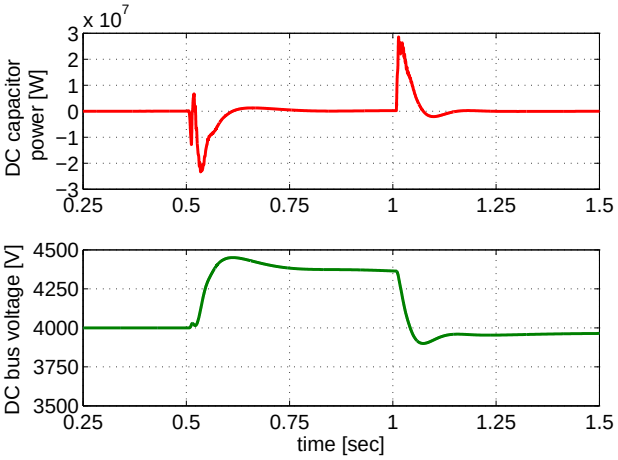

Fig. 17. Capacitor power (upper) and DC bus voltage (lower)

Due to the slow response time chosen for the DC bus voltage control loop, an excess of energy will be stored in the capacitor, increasing it's voltage. The capacitance must be large enough to handle this amount of energy, allowing an adequate decoupling of active power between series and shunt converters. It is also possible to attach a storage system in DC bus for this purpose.

The total injected DC capacitor power and DC bus voltage are shown in Fig.17.

6. CONCLUSION

In this work, a strategy for voltage sag compensation is presented with full voltage restoration with phase jump compensation. Results show a better wind farm performance with the proposed strategy, than that found in magnitude only compensation schemes; the transient fluctuations of electrical current and rotor speed, are lower in the proposed scheme.

Moreover, the proposed strategy does not need converters with higher power rating than that found in other schemes.

Thus, considering the improvement in performance, and the results of the power rating comparison, the proposed strategy is highly recommended in retrofitting the existing Induction Generator based Wind Farms.

ACKNOWLEDGEMENTS

The authors would like to thank to *Fundación YPF*, to La Plata National University – UNLP, to National Agency of Science and Technology Promotion ANPCyT (PICT08/11-0535), and to *Comision Nacional de Investigaciones Científicas – CONICET*, by them financial support.

REFERENCES

M.P. Pálsson, K. Uhlen and J.O.G. Tande. *Large-scale Wind Power Integration and Voltage Stability Limits in Regional Networks* IEEE 2002. p.p. 762–769

Procedimiento de operación de Red Eléctrica de España P.O.12.3 *Requisitos de respuesta frente a huecos de tensión de las instalaciones eólicas* Spanish Utility Operational Procedure

E.ON Netz GmbH. *Grid Code, High and extra high voltage* Bayreuth, Germany. August, 2003.

Z. Saad-Saoud, M.L. Lisboa, J.B. Ekanayake, N. Jenkins and G. Strbac. *Application of STATCOM's to wind farms* IEE Proc. Gen. Trans. Distrib. vol. 145, No. 5; Sept. 1998

P. Ledesma, J. Usaola, J.L. Rodriguez. *Transient stability of a fixed speed wind farm* Renewable Energy 28, 2003 pp.1341–1355

Y. Tai-Her and W. Li *A study on generator capacity for wind turbines under various tower heights and rated wind speeds using weibull distribution* IEEE Trans. Energy Convers., vol. 23, no. 2, pp. 592602, Jun. 2008.

P. Rosas. *Dynamic influences of wind power on the power system* Technical report RISØR-1408. Ørsted Institute. March 2003.

The MathWorks, Inc. *SimPowerSystems Reference* 2007 Available online: www.mathworks.com

P. Kundur. *Power System Stability and Control* McGraw-Hill, 1994. ISBN 0-07-035958-X

R.C. Dugan, M.F. McGranahan, S. Santoso, H.W. Beaty. *Electrical Power Systems Quality* 2nd Edition McGraw–Hill, 2002. ISBN 0-07-138622-X

N.G. Hingorani and L. Gyugyi. *Understanding FACTS* IEEE Press; 2000.

N.G. Hingorani. *Introducing Custom Power* IEEE Spectrum. June1995 pp. 41–48.

A. Ghosh, G. Ledwich. *Power Quality Enhancement Using Custom Power Devices* Kluwer Academic Publisher, 2002. ISBN 1-4020-7180-9

C. Schauder, H. Mehta. *Vector analysis and control of advanced static VAR compensators* IEE PROCEEDINGS-C, Vol.140, No.4, July 1993.

H. Akagi, E.H. Watanabe, M. Aredes *Instantaneous Power Theory and Applications to Power Conditioning* Wiley-IEEE Press, 2007. ISBN 978-0-470-10761-4

E.M. Sasso, G.G. Sotelo, A.A. Ferreira, E.H. Watanabe, M. Aredes and P.G. Barbosa. *Investigação dos Modelos de Circuitos de Sincronismo Trifásicos Baseados na Teoria das Potências Real e Imaginária Instantâneas (p–PLL e q–PLL)* In: Proc. (CDROM) of the CBA 2002 – XIV Congresso Brasileiro de Automtica, pp. 480-485, Natal RN, Brasil, 1-4, Sep. 2002

N.G. Jayanti, M. Basu, M.F. Conlon and K. Gaughan. *Rating requirements of s Unified Power Quality Conditioner (UPQC) fo Voltage Ride Through Capability*

Enhancement 3rd IET International Conference on Power Electronics, Machines and Drives. 2006

Marcelo F. Farias Was born in Villa Gesell, Argentina, in 1975. He received the Engineer degree from La Plata National University, Buenos Aires, Argentina. Currently he is an assistant professor at the Electrical Engineering Department at UNLP. He has worked as a researcher for since 2007. His research interests include power electronics, power quality, and power systems operation and control.

Pedro E. Battaiotto Received the B.S.E.E. degree from National University of La Plata (UNLP), Buenos Aires, Argentina, in 1977. Currently, he is a Full Professor in the Electrical Engineering Department at UNLP, where he has been since 1991. He was Scientific Associate at the European Organization for Nuclear Research (CENR), Switzerland, from 1986 to 1987. He was also Scientific Associate at Microprocessors Lab-INFN-International Center for Theoretical Physics (ICTP), Trieste, Italy, from 1988 to 1989. His primary area of interest is power electronics in energy conversion systems

Marcelo G. Cendoya Was born in La Plata, Argentina, in 1959. received the B.S.E.E. degree from National University of La Plata (UNLP), Buenos Aires, Argentina, in 1987. Received the M.Sc. degree in electrical engineering from the Federal University of Rio de Janeiro, Brazil, in 1992. Currently, he is a assistant Professor in the Electrical Engineering Department at UNLP, where he has been since 2000. His primary area of interest is power electronics in energy conversion systems